JARO 16: 447–457 (2015)
DOI: 10.1007/s10162-015-0524-x

JARO
Journal of the Association for Research in Otolaryngology

Research Article

Stapes Vibration in the Chinchilla Middle Ear: Relation to Behavioral and Auditory-Nerve Thresholds

Luis Robles,[1] Andrei N. Temchin,[2] Yun-Hui Fan,[3] and Mario A. Ruggero[2]

[1]*Instituto de Ciencias Biomédicas (Facultad de Medicina), Universidad de Chile, Santiago, Chile*

[2]*Knowles Hearing Center (Department of Communication Sciences and Disorders), Northwestern University, Evanston, IL, USA*

[3]*iTriage, Denver, CO, USA*

Received: 19 March 2014; Accepted: 17 May 2015; Online publication: 12 June 2015

ABSTRACT

The vibratory responses to tones of the stapes and incus were measured in the middle ears of deeply anesthetized chinchillas using a wide-band acoustic-stimulus system and a laser velocimeter coupled to a microscope. With the laser beam at an angle of about 40 ° relative to the axis of stapes piston-like motion, the sensitivity-vs.-frequency curves of vibrations at the head of the stapes and the incus lenticular process were very similar to each other but larger, in the range 15–30 kHz, than the vibrations of the incus just peripheral to the pedicle. With the laser beam aligned with the axis of piston-like stapes motion, vibrations of the incus just peripheral to its pedicle were very similar to the vibrations of the lenticular process or the stapes head measured at the 40 ° angle. Thus, the pedicle prevents transmission to the stapes of components of incus vibration not aligned with the axis of stapes piston-like motion. The mean magnitude curve of stapes velocities is fairly flat over a wide frequency range, with a mean value of about 0.19 mm·(s Pa^{-1}), has a high-frequency cutoff of 25 kHz (measured at −3 dB re the mean value), and decreases with a slope of about −60 dB/octave at higher frequencies. According to our measurements, the chinchilla middle ear transmits acoustic signals into the cochlea at frequencies exceeding both the bandwidth of responses of auditory-nerve fibers and the upper cutoff of hearing. The phase lags of stapes velocity relative to ear-canal pressure increase approximately linearly, with slopes equivalent to pure delays of about 57–76 μs.

Keywords: middle ear, stapes, incus, chinchilla

INTRODUCTION

The hearing thresholds of mammalian and other tetrapod species are typically relatively flat over a limited frequency span and rise sharply beyond some high frequency (Fay 1988), which largely determines its overall bandwidth. Two of us proposed that the outer and middle ears jointly act as a broadband transmission system and that the high-frequency limit of hearing is imposed by the cochlea (Ruggero and Temchin 2002). Ruggero and Temchin presented strong comparative evidence that "the high-frequency limit of the audiogram in great part is determined internally in the cochlea by the high-frequency arms of the frequency-threshold tuning curves of auditory-nerve fibers with the highest characteristic frequencies." That proposal was inspired by the realization that, in gerbil, stapes velocity (Overstreet and Ruggero 2002) and pressure magnitudes in scala vestibuli (Olson 1998) are relatively constant over a frequency range which substantially exceeds the bandwidth of the gerbil audiogram (see Fig. 3 of (Ruggero and Temchin 2002)). Wide-band middle-ear transmission in gerbil has been subsequently confirmed (Ravicz et al. 2008; Decraemer et al. 2007a; de la Rochefoucauld et al. 2008). The present study was undertaken to establish whether the

Correspondence to: Mario A. Ruggero · Knowles Hearing Center (Department of Communication Sciences and Disorders) · Northwestern University · Evanston, IL, USA. email: mruggero@northwestern.edu

bandwidth of stapes vibration velocity also exceeds the bandwidth of the audiogram in chinchilla.

Among mammals, the chinchilla has an audiogram with a relatively low high-frequency cutoff which makes it an especially convenient species for investigating the influence of middle-ear transmission on hearing. Initial studies (Songer and Rosowski 2007; Ruggero et al. 1990) could not ascertain the high-frequency limit of the transfer function of the chinchilla middle ear because of technical limitations but more recent studies concluded that middle-ear transmission determines the high-frequency cutoff of the audiogram (Slama et al. 2010; Ravicz et al. 2010; Ravicz and Rosowski 2013a, b). The first purpose of the present investigation was to extend our previous measurements of the bandwidth of stapes vibrations in chinchilla (Ruggero et al. 1990) taking advantage of improved acoustic-stimulus and velocity-recording systems. A second purpose was to explore an apparent boost of middle-ear transmission at the pedicle of the chinchilla incus, which we reported at meetings (Ruggero et al. 2004, 2007; Temchin et al. 2002; Robles et al. 2005, 2006).

METHODS

Animal Preparation

All animal experiments were conducted in accordance with a protocol approved by the Animal Care and Use Committee of Northwestern University. Useful data were obtained from 20 male chinchillas (*Chinchilla lanigera*). After sedation with a subcutaneous injection of ketamine HC1 (20 mg/kg), chinchillas were anesthetized with an intraperitoneal injection of dial (50 mg/kg) in urethane (40 mg/kg), later supplemented as needed to maintain deep anesthesia. Rectal temperature was monitored and maintained at 39 °C by means of a servo-controlled battery-powered electrical heating pad. All chinchillas were tracheotomized and intubated to maintain a clear airway. The left pinna was excised, and after opening the auditory bulla widely, the tendon of the tensor tympani muscle was cut and the stapedius muscle was detached from its anchoring. A ball silver-wire electrode was placed on the round window to record compound action potentials evoked by tone bursts that allowed monitoring the physiological state of the middle ear and the cochlea during the experiments. The bony ear canal was opened widely, thus fully exposing the tympanic membrane.

Stimuli and Their Calibration

In 15 chinchillas, measurements were carried out with the laser beam positioned at an angle of approximately 40 ° relative to the axis of stapes piston-like motion (measured in two animals; see Fig. 1), with intact tympanic membrane. In five other chinchillas, the laser beam was directed, through a perforation on the dorsal region of the tympanic membrane, at an angle close to the axis of stapes piston-like motion. The latter measurements sought to ascertain whether the axis of the laser beam relative to the axis of piston-like stapes was somehow related to an apparent boost across the pedicle of the incus in measurements with the laser beam at a 40 ° angle (Ruggero et al. 2007).

Acoustic stimuli were tone bursts, digitally synthesized with a *Tucker-Davis Technologies System II* under computer control and delivered at 80–90 dB SPL via a modified *Radio Shack Super Tweeter 40-1310B* (Chan et al. 1993; Overstreet and Ruggero 2002) either through a closed system or free field (from a position lateral to the tympanic membrane). In the closed system, the tweeter was coupled to a 56-mm-long rubber tube terminated with a speculum tip which abutted against the bone surrounding the tympanic membrane. Sound pressure levels and phases in each ear were measured using a calibrated miniature microphone (*Knowles EK-23133*) coupled to a probe tube with its tip located within 2 mm of the tympanic membrane. [The miniature microphone with its associated probe tube was previously calibrated

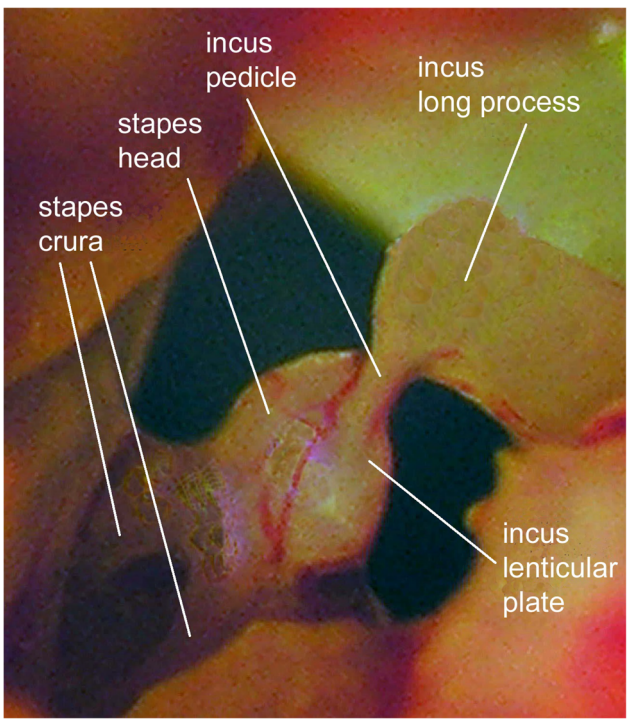

FIG. 1. Coupling between the incus and the stapes in the chinchilla middle ear viewed along an axis inclined about 40 ° relative to the axis of stapes piston-like motion. The long process and the lenticular plate of the incus are connected by the pedicle. The incudo-stapedial joint is constituted by a tight connection between the lenticular plate of the incus and the head of the stapes.

against a 1/8-in. *Brüel & Kjaer* microphone, with the probe-tube tip almost touching the protective grid of the 1/8″ microphone.] The in situ calibrations used an automated adaptive procedure which minimized stimulus levels. The maximal attainable stimulus levels as a function of frequency in the 15 animals in which sound was delivered via the closed system are shown in panel A of Figure 2 for constant and unattenuated voltage inputs to the earphone. The corresponding phases are shown in panels B and C. Pressure-magnitude curves span ranges of about 20 dB for most frequencies below 30 kHz and include a consistent sharp peak at about 37 kHz. Phase curves are roughly similar for all animals, with slopes equivalent to a mean pure delay of about 270 μs (the sum of acoustic, electric, and digital delays in the stimulus system). However, phases varied greatly across animals: the ranges of variability were in the order of two periods at 40 kHz, equivalent to delay differences of 50 μs.

We checked for the existence of ear-canal standing waves (Ravicz and Rosowski 2012) by plotting (panel C) de-trended versions of the phase curves of panel B. [De-trending was carried out by first computing a linear (least-squares) fit to the phase curve and then subtracting it from the phase curve.] Half-period jumps in the de-trended phase curves (panel C) coinciding in frequency with notches in the pressure levels (panel A) would indicate the presence of standing waves that might vitiate velocity recordings from middle-ear ossicles. No such coincidences between half-period phase jumps and amplitude sharp notches were found for frequencies 20–35 kHz, indicating that standing waves did not influence our ossicular-velocity measurements.

Vibration-Data Acquisition

Ossicular vibrations were recorded using a Polytec laser Doppler vibrometer (OFV 3001 Controller, OFV 511 Fiber interferometer) coupled to a compound microscope (Olympus BH2-UMA). The laser beam was directed either through an opening in the auditory bulla (in 15 animals; see Fig. 1) or via a perforation of the tympanic membrane (in 5 animals). The vibrometer received the laser light reflected from one or several glass microbeads (~25 μm diameter) with high index of refraction (Mo Sci Corp., Rolla, MO) placed on the incus long process near the pedicle, the incus lenticular process close to the head of the stapes, or the stapes head itself (Fig. 1). The output of the vibrometer, an electrical voltage proportional to target velocity, was digitized (16-bit resolution, sampling rate of 166 kHz) and stored for offline Fourier analysis using custom MATLAB programs and further processed using

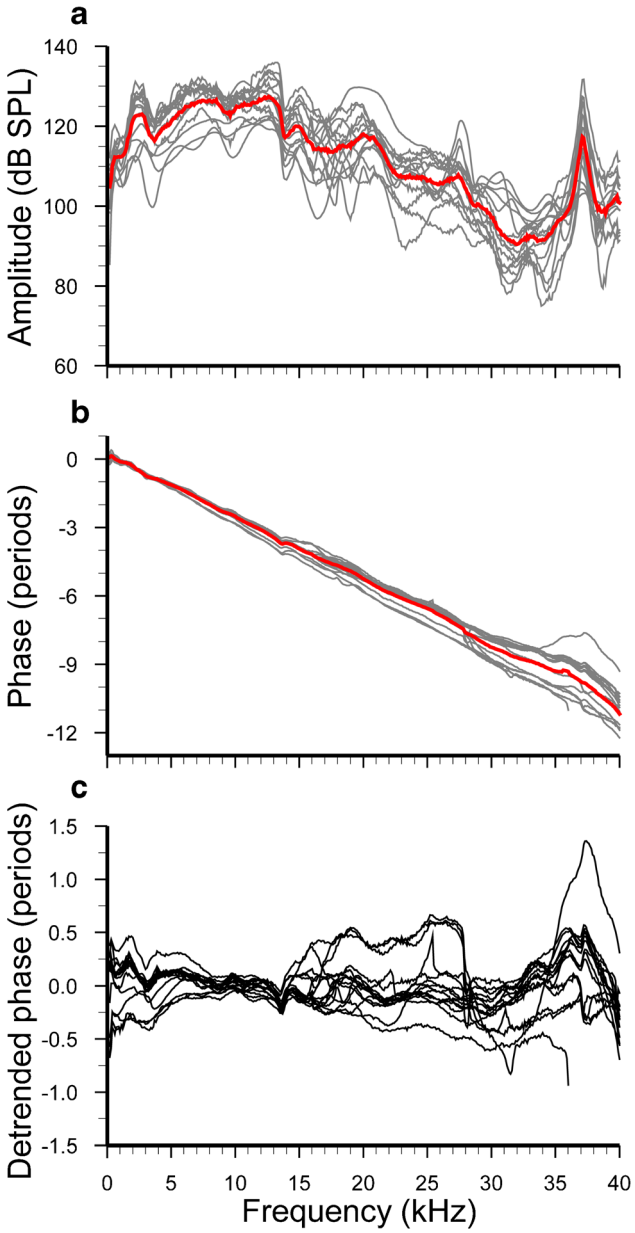

FIG. 2. Stimulus calibrations for the experiments in which ossicular motion was measured with the laser beam positioned at a 40 ° angle relative to the axis of stapes piston-like motion. **A** SPL near the eardrum produced by a constant and unattenuated voltage input to the speaker. **B** Phases of the pressure expressed relative to the voltage input to the speaker. The *thin lines* indicate calibration curves in 15 individual chinchillas and the *thick red line* indicates their mean values. **C** Linear de-trended versions of the individual phase curves. Measurements were obtained at frequencies 0.2–40 kHz, with 100-Hz steps.

EXCEL spreadsheets. In our analysis, we only include data obtained with a signal to noise ratio >20 dB. The mean velocity amplitudes are expressed as log averages (i.e., the means and standard deviations of the logarithms of the velocity amplitudes were computed first and then their antilogarithms were taken). In the figures showing velocity amplitudes and phases, we

present the mean values and the 95 % confidence intervals, computed as two standard errors above and below the means.

RESULTS

Vibration velocity was measured in 20 deeply-anesthetized chinchillas using a laser velocimeter coupled to a microscope. In 15 chinchillas, measurements were always made along an axis of the laser beam differing by about 40 ° from the presumed axis of piston-like stapes motion. [Measurements in five other chinchillas, described below, were made along an axis closely approximating that of stapes piston-like motion; see Fig. 5]. Figure 1 shows the incus and the stapes as viewed along the axis of the microscope objective in the 15 experiments carried out at a 40 ° angle. In chinchilla, as in other species, the long process and the lenticular plate of the incus are connected by a fine bony structure, the pedicle; the incudo-stapedial joint consists of a close apposition of the incus lenticular plate and the stapes head (see (Funnell et al. 2005)). Vibrations of both the long process and the lenticular plate of the incus were measured in those 15 chinchillas. The vibrations of the stapes head (near the edge of the lenticular plate) were also measured in 5 of the 15 chinchillas. No significant differences were found between the motions of the stapes head and the incus lenticular plate (Robles et al. 2006; Ruggero et al. 2007). In the remainder of the paper, for measurements at both 40 ° and 0 ° angles, the velocity of the lenticular plate is reported as "velocity of the head of the stapes" (following (de la Rochefoucauld et al. 2008)).

Figure 3 shows the individual magnitudes and phases of the stapes-head velocity responses to tones presented at 80–90 dB SPL, referred to ear-canal stimulus pressure (i.e., with units of velocity per Pascal) in 15 chinchilla ears and plotted against frequency. Both the magnitudes and phases exhibit substantial dispersion, which increases with frequency (e.g., phases scattered over 2 cycles, equivalent to almost 70 microseconds, at 30 kHz). The velocity magnitudes (Fig. 3A) are relatively flat and similar up to at least 20 kHz but exhibit peaks and troughs and greater variability at higher frequencies. The stapes-velocity phases (Fig. 3B) show lags that increase approximately linearly.

Figure 4 displays the mean values and the 95 % confidence intervals of the stapes velocity magnitudes and phases of Figure 3. In the case of magnitudes, the logarithmic averages are displayed (see "METHODS"). The stapes velocities are shown plotted on linear frequency scales in panels A and B and,

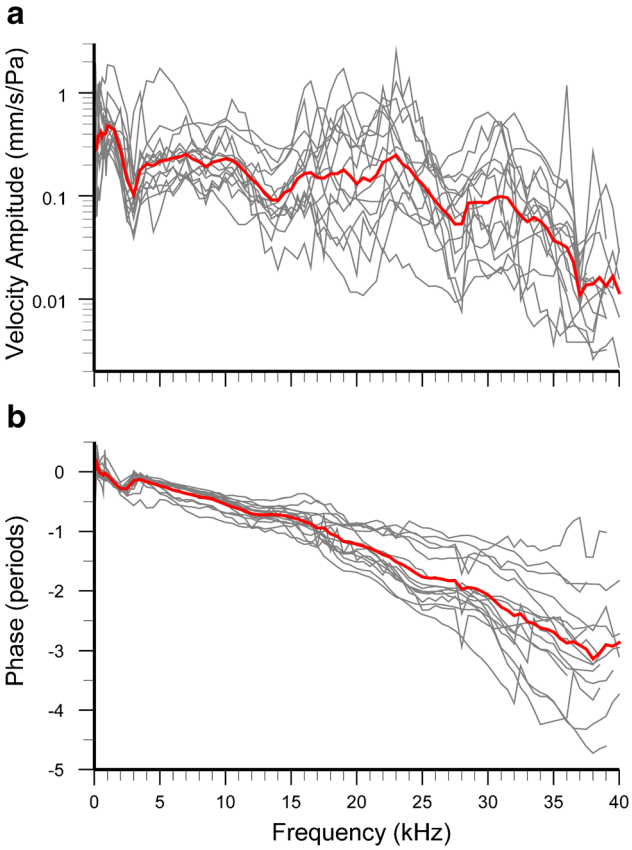

FIG. 3. Stapes-velocity magnitudes (**A**) and phases (**B**) referred to ear-canal stimulus pressure as a function of frequency. The *thin lines* display the magnitudes (peak instantaneous amplitudes) and phases of the stapes velocity measured in 15 chinchillas in which ossicular motion was measured with the laser beam positioned at a 40 ° angle relative to the axis of stapes piston-like motion. *Thick red lines*: logarithmic average of the velocity magnitudes (**A**) and mean of the velocity phases (**B**). Measurements were obtained at frequencies 0.1–1 kHz, with 100-Hz steps, and 1–40 kHz, with 500-Hz steps.

to permit a more detailed view of low frequencies, on logarithmic frequency scales in panels C and D. The mean stapes-velocity magnitude curves (A and C) are fairly flat over a wider frequency range than the individual curves (Fig. 3A). Their average, computed between 0.5 and 25 kHz (dashed black line in Fig. 4C), is 0.19 mm·(s Pa^{-1}) and their high-frequency cutoff [measured at 0.13 mm·(s Pa^{-1}), i.e., −3 dB relative to the average] is 25 kHz. For frequencies higher than 25 kHz, stapes velocity magnitude decreases with a slope of about −60 dB/octave (oblique dashed line in panel C). The range of the 95 % confidence interval is within 10 dB for frequencies up to 15 kHz and within 20 dB for almost all frequencies. The mean stapes-velocity phases increasingly lag with frequency, with a slope corresponding to a delay of about 57 μs for frequencies up to 15 kHz and about 76 μs for frequencies up to 25 kHz. The range of the 95 % confidence interval is

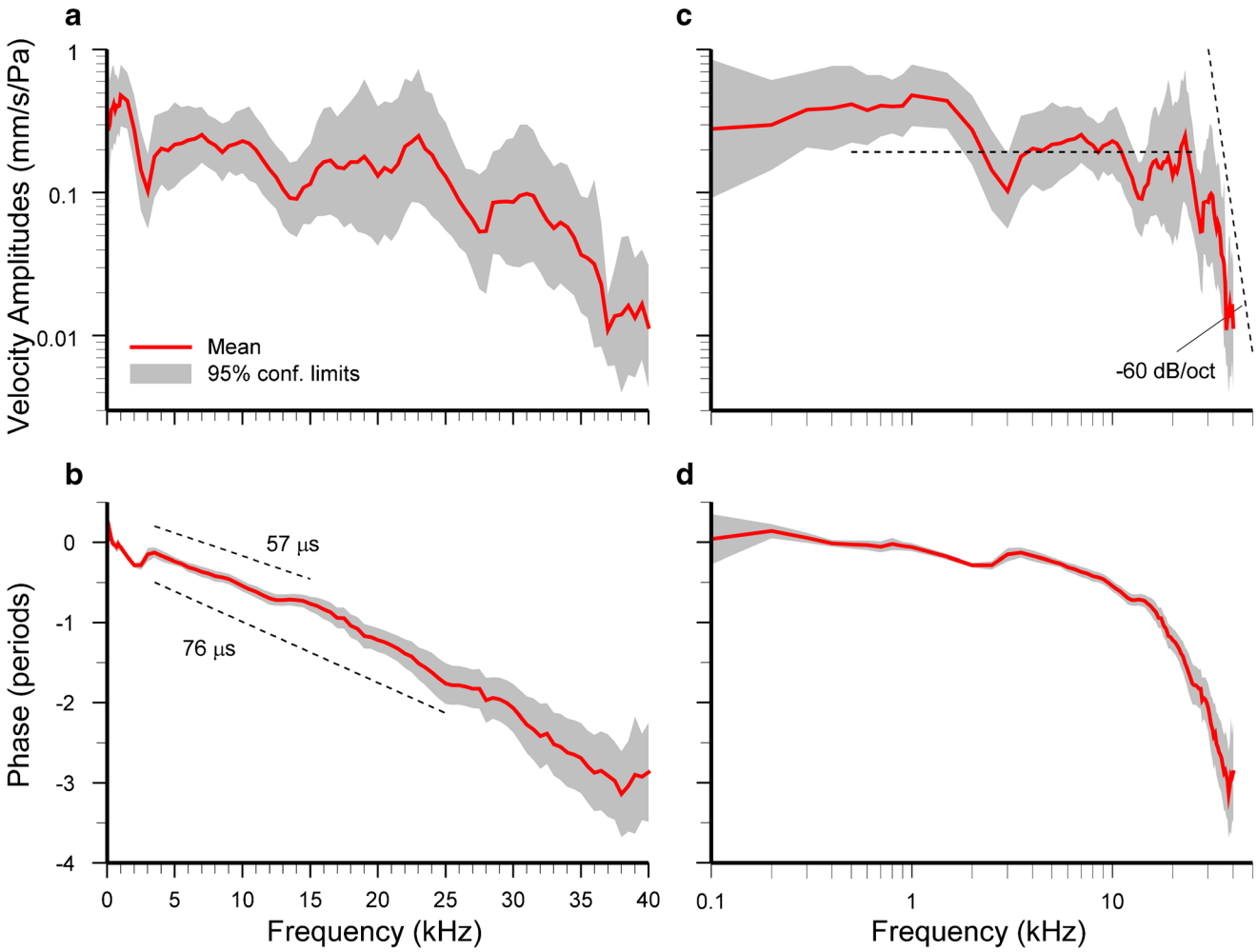

FIG. 4. Mean values of stapes-velocity magnitudes and phases referred to ear-canal stimulus pressure plotted against linear frequency (**A**, **B**, respectively) and logarithmic frequency (**C**, **D**, respectively). The curves for velocity magnitudes, peak instantaneous amplitudes (*red solid lines*), represent logarithmic averages (see "METHODS") computed from the individual curves of Figure 3. The *shaded areas* display the 95 % confidence intervals of stapes-velocity magnitudes and phases. The *horizontal black dashed line* in panel **C** represents the mean velocity magnitude in the frequency range 0.5–25 kHz. The *straight dashed lines* in **B** have constant slopes corresponding to delays of 57 and 76 µs. The *oblique dashed line* in **C** has a slope of −60 dB/octave.

within 0.18 periods for frequencies up to 15 kHz and within 0.5 periods for frequencies up to 25 kHz.

The vibration velocity of the long process of the incus at a point just distal to the pedicle was measured, with the laser beam at a 40 ° angle, in the same chinchillas for which stapes vibrations are shown in Figures 3 and 4. Between 15 and 30 kHz (Fig. 5A), the average magnitudes of incus vibrations (blue trace) were smaller than those of stapes velocity (red trace), hinting at a boost of transmission at the incus pedicle, between the long and lenticular processes, as previously reported (Robles et al. 2006; Ruggero et al. 2007). To explore this issue, we measured ossicular vibrations in five other chinchillas using free-field stimulation, with the laser beam directed (through a perforation made on the dorsal region of the tympanic membrane) at an angle close to the axis of stapes piston-like motion. Figure 5A shows average sensitivity curves, obtained at the angle close to the axis of stapes piston-like motion, for vibrations of the head of the stapes (in three ears; brown trace) and of the long process of the incus (in five ears; green trace). The stapes and incus curves are similar to each other and are also similar to the average stapes-sensitivity curve measured with the laser beam positioned at a 40 ° angle (red trace). In contrast, they differ substantially from the 40 ° average incus-sensitivity curve (blue trace). Likewise, the average stapes- and incus-velocity phases obtained at an angle close to the axis of stapes piston-like motion are similar to the average stapes-velocity curve obtained at a 40 ° angle and

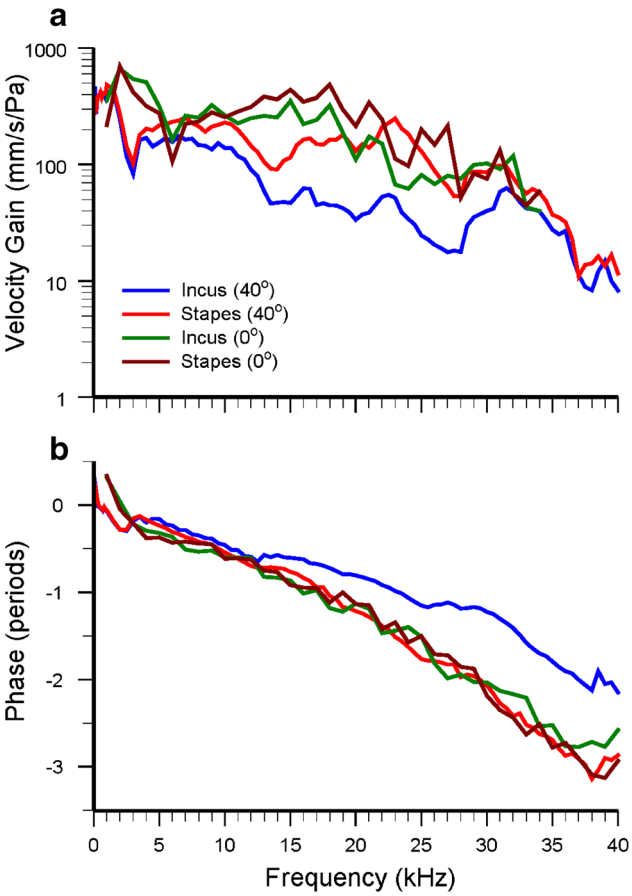

FIG. 5. Comparison of stapes and incus vibrations measured approximately along the axis of stapes piston-like motion and at an angle of about 40 °. **A** Peak instantaneous amplitudes (velocity per unit pressure). **B** Phases (periods). Curves for stapes and incus vibration along the axis of stapes piston-like motion are averages of three and five measurements, respectively, using free-field stimulation and 1-kHz frequency steps. Measurements at an angle of 40 ° were carried out in 15 other ears (same data as in Figs. 3A and 4A, C) using a closed cavity terminated with a speculum tip which abutted against the bone surrounding the tympanic membrane.

substantially different from the 40 ° average incus velocity phases (Fig. 5B).

DISCUSSION

No Boost of Transmission Across the Incus Pedicle

The present results (Fig. 5) dispute the existence of a frequency-dependent boost of transmission across the pedicle of the chinchilla incus reported by (Robles et al. 2006; Ruggero et al. 2007). Such boost, although consistent with differences in motion between the malleus and stapes in the horseshoe bat (Wilson and Bruns 1983), was not found in gerbils, cats, or humans (Decraemer et al. 2007b; de la Rochefoucauld et al. 2008, 2010). We ascribe the apparent boost, observable in Figure 5, to an artifact of unknown origin perhaps related to the (wide, 40 °) angle between the axes of the laser beam and of piston-like stapes motion. The comparison between measurements performed on-axis and at a 40 ° angle (Fig. 5) suggests that at certain frequencies (15–30 kHz), the vibration of the long process of the incus includes a substantial component along an axis different from that of the piston-like motion of the stapes. In other words, far from boosting vibrations transmitted to the stapes, the incus pedicle appears to insulate the stapes from non-piston-like motion, as suggested by a finite-element model of the cat middle ear ((Funnell et al. 2005); also discussed by (Elkhouri et al. 2006)). Three-dimensional stapes velocity measurements in gerbil (Decraemer et al. 2007a; Ravicz et al. 2008) reveal predominantly piston-like stapes motion but also substantial transverse (tilting-like) components at some frequencies. It is not clear whether these contribute significantly to generate pressure in scala vestibuli (Edom et al. 2013).

Stapes Velocity in the Present Study and Others

Ravicz and Rosowski (2013b) recently reviewed the literature of chinchilla stapes-velocity transfer functions and found them to be generally similar (Ruggero et al. 1990; Songer and Rosowski 2006; Slama et al. 2010; Koka et al. 2010; Ravicz and Rosowski 2013b). All but two of the then available stapes-velocity transfer functions were limited to frequencies <20 kHz (see Fig. 7 of (Ravicz and Rosowski 2013b)). Figure 6A compares those two transfer functions, which extend to frequencies ≥20 kHz (magenta and blue traces; (Slama et al. 2010; Ravicz and Rosowski 2013b)), with the present stapes-velocity magnitude curve (red trace; from Figs. 3 and 4 but expressed in root-mean-square units). All three velocity curves include notches at 2–3 kHz and are otherwise similar both in shape and absolute magnitudes up to 6–10 kHz. Beyond those frequencies, the red curve (present work) remains relatively flat up to about 30 kHz, the blue curve (Ravicz and Rosowski 2013b) decays rapidly, and the magenta curve hovers irregularly between the other two curves. The stapes-velocity phases (Fig. 6B) are similar for frequencies up to 10 kHz and diverge at higher frequencies.

The present results and those of (Ravicz and Rosowski 2013b) stand in clear disagreement at frequencies >10 kHz. In no small part, the differences between velocity transfer functions arise from differences in the stimulus-pressure calibrations of the two studies. In particular, Ravicz and Rosowski found that a prominent standing-wave notch exists at frequencies 20–30 kHz within about 1 mm from the chinchilla tympanic membrane (Ravicz and Rosowski 2012) and

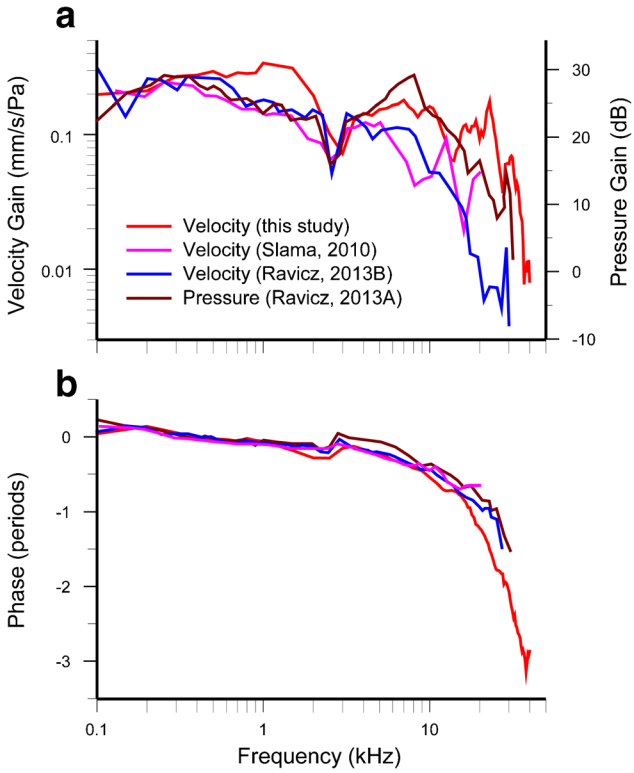

FIG. 6. Comparison of stapes-velocity transfer functions re ear-canal stimulus pressure and middle-ear gain (pressure in scala vestibuli re ear-canal pressure) in chinchilla. **A** Root-mean-square amplitudes. **B** Phases. *Red trace*: stapes velocity from Figure 4. *Magenta trace*: stapes velocity from Fig. 4A of (Slama et al. 2010). *Blue trace*: stapes velocity from Fig. 4A of (Ravicz and Rosowski 2013b). *Brown trace*: middle-ear pressure gain from Fig. 5B of (Ravicz and Rosowski 2013a).

corrected their "raw" stapes velocity measurements using an ear-canal-pressure model (Ravicz and Rosowski 2013a), yielding a velocity transfer function which was attenuated at high frequencies (see Fig. 4A of (Ravicz and Rosowski 2013b)). We did not carry out a comparable correction because we found no clear evidence for standing waves in the 20–30-kHz frequency range (see METHODS and (Fig. 2)). The apparent absence of standing waves in the frequency range 20–30 kHz in chinchilla is consistent with findings in gerbil (Ravicz et al. (2007)): "at frequencies below 30 kHz the (longitudinal) spatial dependence of the measured sound pressure is small" (p. 2165 of (Ravicz et al. 2007)).

At face value, the wide bandwidth and the approximately linear phase-frequency characteristics of the average stapes-velocity transfer function in the present study resemble those of a lossless transmission line, as suggested for other species (Wilson and Bruns 1983; Puria and Allen 1998; Olson 1998; Overstreet and Ruggero 2002). Alternatively, the same characteristics could be produced by a combination of multiple resonances in the tympanic membrane (Fay et al. 2006). Since the middle ear seems to behave as a minimum-phase system (see Figs. 5 and 6 of (Ruggero et al. 1990)), one might expect that the wider bandwidth of the present stapes-velocity measurements (Fig. 6A) should be associated with shorter phase delays than in previous measurements (Slama et al. 2010; Ravicz and Rosowski 2013b). However, the present phase delays are longer than those of previous measurements (Fig. 6B) in the frequency range 20–30 kHz, where magnitudes begin their rapid terminal decay (red trace in Fig. 6A), with a slope of −60 dB/octave (Fig. 4C). This association of longer phase delays with abrupt changes of magnitude slopes is consistent with minimum-phase behavior (Bode 1945).

Middle-Ear Pressure Gain

The immediate input to the cochlea is not stapes velocity but rather the pressure that it generates in scala vestibuli. Therefore, the ratio between scala-vestibuli pressure (P_{SV}) and pressure at the tympanic membrane, i.e., the so-called middle-ear pressure gain (G_{MEP}), may be viewed as a measure of middle-ear transmission.

$$G_{MEP} = P_{SV}/P_{TM}$$

Middle-ear pressure gains have been measured in chinchilla by Décory et al. (1990), Ravicz et al. (2010), Slama et al. (2010), and Ravicz and Rosowski (2013a). Interestingly, the G_{ME} magnitude curve reported by (Ravicz and Rosowski 2013a), shown in Figure 6 (brown trace), has a high-frequency cutoff close to that of the present stapes-velocity magnitudes (red trace) and also substantially higher than the corresponding stapes-velocity measurements made by the same authors (blue trace (Ravicz and Rosowski 2013b); magenta trace (Slama et al. 2010)).

It is noteworthy that both the "raw" mean G_{ME} (see Figs. 2A and 5B of (Ravicz and Rosowski 2013a)) and the raw mean stapes-velocity transfer function (Fig. 4A of (Ravicz and Rosowski 2013b)) actually have bandwidths not too dissimilar from that of the present stapes-velocity curve. It is only after corrections (to compensate for the apparent existence of standing waves) were applied that the bandwidths became sharply restricted, possibly reflecting an over-correction based on an ear-canal model (Ravicz and Rosowski 2012) or the influence of errors in pressure-sensor calibrations (Ravicz et al. 2010; Ravicz and Rosowski 2013a).

The Bandwidths of Stapes-Velocity Magnitudes, Auditory-Nerve Thresholds, and Behavioral Thresholds

Figure 7 compares stapes-vibration sensitivity (Figs. 3 and 4) with the sensitivity of high spontaneous rate chinchilla auditory-nerve fibers (brown trace), computed from characteristic frequency average-rate thresholds (Temchin et al. 2008b). Auditory-nerve fibers in chinchilla appear to respond roughly in proportion to a weighted combination of basilar-membrane displacement and velocity rather than solely displacement (Narayan et al. 1998; Ruggero et al. 2000). Specifically, good matches were found between auditory-nerve fiber frequency-threshold tuning curves and tuning curves for basilar-membrane displacements high-pass filtered at an average rate of 4 dB/octave (Narayan et al. 1998). Hence, the blue trace of Figure 7 shows a modified neural-sensitivity curve obtained by low-pass filtering the brown curve at a rate of −4 dB/octave. Thus, the modified auditory-nerve sensitivity curve should approximate the frequency dependence of basilar-membrane displacement and, hence, of stapes velocity. [Note that at least for frequencies 150–2000 Hz at the base of the chinchilla cochlea, basilar-membrane displacement is proportional to, and in phase with, velocity (rather than displacement) of the stapes (Ruggero et al. 1990).] Indeed, as Figure 7 shows, the stapes-velocity and the modified neural-sensitivity curves are similar over nearly a two-decade frequency range (200 Hz–14 kHz), mostly differing in that the neural curve shows no evidence of a counterpart to the prominent 3-kHz notch in the stapes-velocity curve, which is also evident in other middle-ear measurements ((Rosowski et al. 2006; Ravicz and Rosowski 2013b)). The absence of a notch in the average neural data may be due to individual variations in the sizes of bulla openings. Such variations should lead to shifts in the notch frequency (Rosowski et al. 2006), causing the notch to be "washed-out" upon averaging. What is clear from Figure 7 is that the high-frequency cutoff of stapes-velocity sensitivity obtained in the present study (red trace) is nearly an octave higher than the cutoff of auditory-nerve fiber responses (if evaluated at −15 dB in both cases). Thus, it is the intrinsic mechanical properties of the cochlea, i.e., tonotopicity at its base [which, in turn, largely determine the responses of auditory-nerve fibers (Narayan et al. 1998; Ruggero et al. 2000)], rather than the input to the cochlea (middle-ear vibrations), which limit the upper cutoff of hearing ((Ruggero and Temchin 2002); see especially their Figures 4 and 5 and accompanying text).

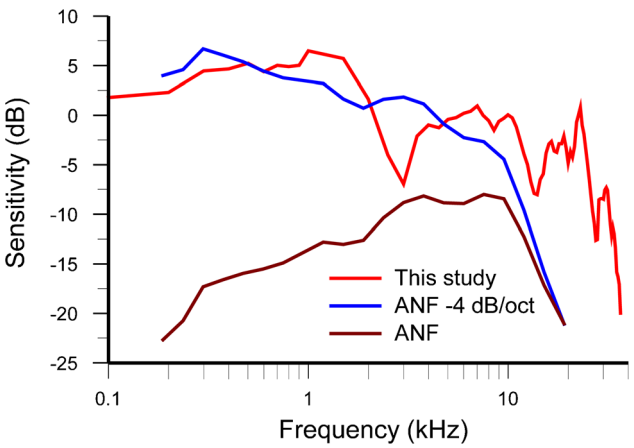

FIG. 7. Comparison of the frequency dependence of stapes-vibration velocity and auditory-nerve sensitivity in chinchilla. The sensitivity references ("0 dB" in the ordinate) are arbitrary. Stapes-vibration velocity is as shown in Figure 4C. Two curves are shown for auditory-nerve sensitivity. The *brown trace* corresponds to characteristic-frequency average-rate thresholds of auditory-nerve fibers with high spontaneous activity (Temchin et al. 2008a). Auditory-nerve fibers appear to respond in proportion to, and in phase with, a combination of basilar-membrane displacement and velocity rather than solely displacement (Narayan et al. 1998; Ruggero et al. 2000). Specifically, Narayan et al. (1998) found that frequency-threshold tuning curves of auditory-nerve fibers best matched tuning curves of basilar-membrane vibrations for displacements high-pass filtered at an average rate of 4 dB/octave. Accordingly, the *blue trace* is a modified version of the *brown trace*, obtained by first low-pass filtering the latter at a rate of −4 dB/octave and then displacing the resultant to make it coincide with the *brown curve* at 19 kHz.

Figure 8 compares stapes-vibration sensitivity (from this study and from Fig. 4A of (Ravicz and Rosowski 2013b)) with behavioral (Miller 1970; Heffner and Heffner 1991) and auditory-nerve sensitivities (Temchin et al. 2008b) in chinchilla. To make stapes-velocity and auditory-nerve sensitivities (expressed re SPL at the eardrum) comparable to behavioral sensitivities (measured in intact chinchillas in a free field), they have been corrected according to the external-ear transfer function (Fig. 9A of (von Bismarck 1967); see also (Murphy and Davis 1998)) and the differences between stapes-velocity magnitudes (and, hence, auditory-nerve thresholds) with open and closed bulla (Fig. 10 of (Ruggero et al. 1990)). Additionally, the corrected velocity curves have been displaced vertically to optimally match Miller's behavioral audiogram at frequencies <2 kHz. Auditory-nerve sensitivity is represented by two brown traces: a solid line, computed from average-rate thresholds, and a dashed line, computed from the same thresholds but shifted upward by 15 dB for frequencies <1.5 kHz [and by lower values for frequencies up to 4.5 kHz, based on Fig. 7 of (Temchin and Ruggero 2010)]. This acknowledges the possibility that hearing thresholds at those frequencies are set by phase-locking thresholds ((Javel et al. 1988); p. 529), which are about 15 dB lower than average-rate thresholds (Johnson 1980). The stapes-velocity and

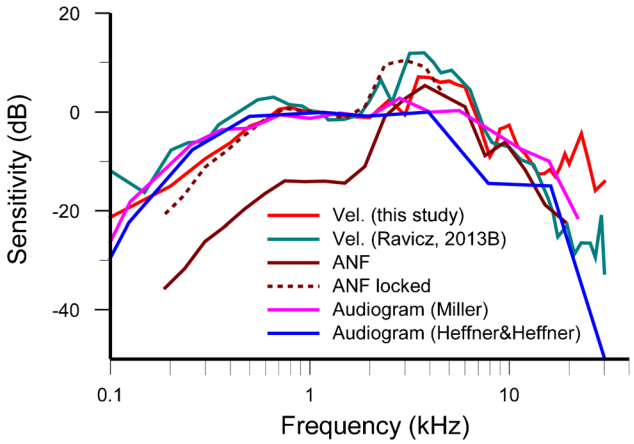

FIG. 8. Comparison of the frequency dependence of stapes-vibration velocity, auditory-nerve sensitivity, and behavioral thresholds measured in free field in chinchilla (*blue line*: (Heffner and Heffner 1991); *magenta line*: (Miller 1970)). Stapes-vibration velocity curves (*red trace* from Fig. 4C and *green trace form* (Ravicz and Rosowski 2013b)) and auditory-nerve sensitivity (*solid brown trace*), all originally referred to sound pressure at the tympanic membrane and obtained with an open bulla, have been corrected using an external-ear transfer function for chinchilla (von Bismarck 1967) and also (for frequencies between 100 and 700 Hz) by a correction factor derived from stapes velocity measurements with open and closed bulla in chinchilla (Fig. 10 of (Ruggero et al. 1990)). Auditory-nerve sensitivity is also shown shifted upward by 15 dB for frequencies <1.5 kHz (*brown-dash trace*) to acknowledge the possibility that hearing thresholds at those frequencies are set by auditory-nerve phase-locking (Johnson 1980) rather than average rate ((Javel et al. 1988); p. 529).

the (phase-locking corrected) auditory-nerve curves are similar to the audiograms at frequencies lower than 2 kHz but exceed their sensitivity between 2 and 7 kHz by as much as 10 dB. Between 7 and 16 kHz, the stapes-velocity curves are close to Miller's audiogram but consistently exceed the audiogram of (Heffner and Heffner 1991). At frequencies >16 kHz, both behavioral audiograms plummet while the present stapes-velocity curve (red trace) remains relatively constant. If measured at −15 dB, the high-frequency cutoff of stapes velocity is higher than 25 kHz, whereas the cutoffs are 8 and 18 kHz for the audiograms of Heffner and Heffner and Miller, respectively, and 13 kHz for auditory-nerve sensitivity.

One possible explanation for the difference between the corrected stapes-velocity curves and the audiograms in the range 2–7 kHz is an overcorrection of stapes-velocity magnitudes. However, this seems unlikely because the external-ear transfer function used here (von Bismarck 1967) was replicated in most respects by (Murphy and Davis 1998). The similarity between the stapes-velocity and (phase-locking corrected) auditory-nerve curves at frequencies lower than 10 kHz suggest that hearing thresholds reflect different aspects of auditory-nerve fiber responses in different frequency regions: average-rates at frequencies >2–3 kHz and phase-locking at lower frequencies (Javel et al. 1988).

Summary of Findings and Conclusions

1. The vibratory responses to tones of the stapes and the incus were measured in the middle ears of deeply anesthetized chinchillas using a laser vibrometer.
2. With the axis of the laser beam at an angle of about 40 ° relative to the axis of stapes piston-like motion, the sensitivity-vs.-frequency curves of the head of the stapes and the incus lenticular process were very similar but larger, in the range 15–30 kHz, than the vibrations of the incus just peripheral to the pedicle. In contrast, with the laser beam aligned with the axis of piston-like stapes motion, vibrations of the incus just peripheral to its pedicle were very similar to the vibrations of the incus lenticular process or the stapes head in the same ears and also similar to the vibrations of the stapes measured at a 40 ° angle. We conclude that the apparent transmission boost across the pedicle measured at a 40 ° angle with the axis of stapes piston-like motion is an artifact.
3. The average magnitudes of stapes velocities are fairly similar over a wide frequency range, with a mean value of about 0.19 mm·(s Pa^{-1}) and a high-frequency cutoff of 25 kHz (measured at −3 dB re the mean value), and decrease with a slope of about −60 dB/octave at higher frequencies.
4. The frequency-sensitivity curves of stapes velocity and of auditory-nerve fiber thresholds modified by low-pass filtering (4 dB/octave) to take into account their proportionality to a combination of basilar-membrane displacement and velocity are similar up to about 13 kHz but diverge sharply at higher frequencies, so that the high-frequency cutoff of stapes-velocity sensitivity is nearly an octave higher than the cutoff of auditory-nerve fiber responses. Thus, it is the intrinsic mechanical properties of the cochlea, rather than its input (middle-ear vibrations), which limit the upper cutoff of hearing.
5. The high-frequency cutoff of stapes-velocity sensitivity amply exceeds (by at least 10 kHz) that of the behavioral audiogram.

ACKNOWLEDGMENTS

This work was supported by Grant DC-000419 from the National Institute on Deafness and Other Communication

Disorders. L.R. was partially funded by Grant Fondecyt 1120256 (Chile).

REFERENCES

BODE HW (1945) Network analysis and feedback amplifier design. D. Van Nostrand Company, Inc, New York

CHAN JC, MUSICANT AD, HIND JE (1993) An insert earphone system for delivery of spectrally shaped signals for physiological studies. J Acoust Soc Am 93:1496–1501

DÉCORY L, FRANKE RB, DANCER AL (1990) Measurement of the middle ear transfer function in cat, chinchilla and guinea pig. In: The Mechanics and Biophysics of Hearing (Dallos P, Geisler CD, Matthews JW, Ruggero MA, Steele CR, eds), pp 270-277. Berlin: Springer.

DE LA ROCHEFOUCAULD O, DECRAEMER WF, KHANNA SM, OLSON ES (2008) Simultaneous measurements of ossicular velocity and intracochlear pressure leading to the cochlear input impedance in gerbil. J Assoc Res Otolaryngol 9:161–177

DE LA ROCHEFOUCAULD O, KACHROO P, OLSON ES (2010) Ossicular motion related to middle ear transmission delay in gerbil. Hear Res 270:158–172

DECRAEMER WF, DE LA ROCHEFOUCAULD O, DONG W, KHANNA SM, DIRCKX JJ, OLSON ES (2007A) Scala vestibuli pressure and three-dimensional stapes velocity measured in direct succession in gerbil. J Acoust Soc Am 121:2774–2791

DECRAEMER WF, DE LA ROCHEFOUCAULD O, KHANNA SM, DIRCKX JJJ (2007B) The pedicle of lenticular process in gerbil, cat and human does not produce a boost at the high frequency limit of the audible range. Assoc Res Otolaryngol Midwinter Meet Abstr 30:182

EDOM E, OBRIST D, HENNIGER R, KLEISER L, SIM JH, HUBER AM (2013) The effect of rocking stapes motions on the cochlear fluid flow and on the basilar membrane motion. J Acoust Soc Am 134:3749–3758

ELKHOURI N, LIU H, FUNNELL WR (2006) Low-frequency finite-element modeling of the gerbil middle ear. J Assoc Res Otolaryngol JARO 7:399–411

FAY RR (1988) Hearing in vertebrates: a psychophysics databook. Hill-Fay Associates, Winnetka

FAY JP, PURIA S, STEELE CR (2006) The discordant eardrum. Proc Natl Acad Sci U S A 103:19743–19748

FUNNELL WR, SIAH TH, MCKEE MD, DANIEL SJ, DECRAEMER WF (2005) On the coupling between the incus and the stapes in the cat. J Assoc Res Otolaryngol JARO 6:9–18

HEFFNER RS, HEFFNER HE (1991) Behavioral hearing range of the chinchilla. Hear Res 52:13–16

JAVEL E, MCGEE JA, HORST JW, FARLEY GR (1988) Temporal mechanisms in auditory stimulus coding. In: Edelman GM, Gall WE, Cowan WM (eds) Auditory function—neurobiological bases of hearing. Wiley, New York, pp 515–548

JOHNSON DH (1980) The relationship between spike rate and synchrony in responses of auditory-nerve fibers to single tones. J Acoust Soc Am 68:1115–1122

KOKA K, HOLLAND NJ, LUPO JE, JENKINS HA, TOLLIN DJ (2010) Electrocochleographic and mechanical assessment of round window stimulation with an active middle ear prosthesis. Hear Res 263:128–137

MILLER J (1970) Audibility curve of the chinchilla. J Acoust Soc Am 48:513–523

MURPHY WJ, DAVIS RR (1998) The role of the chinchilla pinna and ear canal in electrophysiological measures of hearing thresholds. J Acoust Soc Am 103:1951–1956

NARAYAN SS, TEMCHIN AN, RECIO A, RUGGERO MA (1998) Frequency tuning of basilar membrane and auditory nerve fibers in the same cochleae. Science 282:1882–1884

OLSON ES (1998) Observing middle and inner ear mechanics with novel intracochlear pressure sensors. J Acoust Soc Am 103:3445–3463

OVERSTREET EH, RUGGERO MA (2002) Development of wide-band middle ear transmission in the Mongolian gerbil. J Acoust Soc Am 111:261–270

PURIA S, ALLEN JB (1998) Measurements and model of the cat middle ear: evidence of tympanic membrane acoustic delay. J Acoust Soc Am 104:3463–3481

RAVICZ ME, ROSOWSKI JJ (2012) Chinchilla middle-ear admittance and sound power: high-frequency estimates and effects of inner-ear modifications. J Acoust Soc Am 132:2437–2454

RAVICZ ME, ROSOWSKI JJ (2013A) Inner-ear sound pressures near the base of the cochlea in chinchilla: further investigation. J Acoust Soc Am 133:2208–2223

RAVICZ ME, ROSOWSKI JJ (2013B) Middle-ear velocity transfer function, cochlear input immittance, and middle-ear efficiency in chinchilla. J Acoust Soc Am 134:2852–2865

RAVICZ ME, OLSON ES, ROSOWSKI JJ (2007) Sound pressure distribution and power flow within the gerbil ear canal from 100 Hz to 80 kHz. J Acoust Soc Am 122:2154–2173

RAVICZ ME, COOPER NP, ROSOWSKI JJ (2008) Gerbil middle-ear sound transmission from 100 Hz to 60 kHz. J Acoust Soc Am 124:363–380

RAVICZ ME, SLAMA MC, ROSOWSKI JJ (2010) Middle-ear pressure gain and cochlear partition differential pressure in chinchilla. Hear Res 263:16–25

ROBLES L, TEMCHIN AN, FAN Y-H, RUGGERO MA (2005) Boost of transmission at the incudo-stapedial joint of chinchilla middle ear. Assoc Res Otolaryngol Midwinter Meet Abstr 28:321–322

ROBLES L, TEMCHIN AN, FAN Y-H, CAI H, RUGGERO MA (2006) Vibrations of the stapes and the long and lenticular processes of the incus in the chinchilla middle ear. Assoc Res Otolaryngol Midwinter Meet Abstr 29:215

ROSOWSKI JJ, RAVICZ ME, SONGER JE (2006) Structures that contribute to middle-ear admittance in chinchilla. J Comp Physiol Neuroethol Sens Neural Behav Physiol 192:1287–1311

RUGGERO MA, TEMCHIN AN (2002) The roles of the external, middle, and inner ears in determining the bandwidth of hearing. Proc Natl Acad Sci U S A 99:13206–13210

RUGGERO MA, RICH NC, ROBLES L, SHIVAPUJA BG (1990) Middle-ear response in the chinchilla and its relationship to mechanics at the base of the cochlea. J Acoust Soc Am 87:1612–1629

RUGGERO MA, NARAYAN SS, TEMCHIN AN, RECIO A (2000) Mechanical bases of frequency tuning and neural excitation at the base of the cochlea: comparison of basilar-membrane vibrations and auditory-nerve-fiber responses in chinchilla. Proc Natl Acad Sci U S A 97:11744–11750

RUGGERO MA, TEMCHIN AN, ROBLES L, OVERSTREET EH (2004) A new and improved middle ear. Proceedings of the 3rd Symposium on Middle Ear Mechanics in Research and Otology 134–141

RUGGERO MA, TEMCHIN AN, FAN YH, CAI HX, ROBLES L (2007) Boost of Transmission at the Pedicle of the Incus in the Chinchilla Middle Ear. In: Middle Ear Mechanics in Research and Otology (Huber A, Eiber A, eds), pp 154-157. Singapore: World Scientific.

SLAMA MC, RAVICZ ME, ROSOWSKI JJ (2010) Middle ear function and cochlear input impedance in chinchilla. J Acoust Soc Am 127:1397–1410

SONGER JE, ROSOWSKI JJ (2006) The effect of superior-canal opening on middle-ear input admittance and air-conducted stapes velocity in chinchilla. J Acoust Soc Am 120:258–269

SONGER JE, ROSOWSKI JJ (2007) Transmission matrix analysis of the chinchilla middle ear. J Acoust Soc Am 122:932–942

TEMCHIN AN, RUGGERO MA (2010) Phase-locked responses to tones of chinchilla auditory nerve fibers: implications for apical cochlear mechanics. Jaro J Assoc Res Otolaryngol 11:297–318

TEMCHIN AN, ROBLES L, RUGGERO MA (2002) A re-examination of middle-ear transmission in chinchilla. Assoc Res Otolaryngol Midwinter Meet Abstr 25:154

TEMCHIN AN, RICH NC, RUGGERO MA (2008A) Threshold tuning curves of chinchilla auditory-nerve fibers. I. Dependence on characteristic frequency and relation to the magnitudes of cochlear vibrations. J Neurophysiol 100:2889–2898

TEMCHIN AN, RICH NC, RUGGERO MA (2008B) Threshold tuning curves of chinchilla auditory nerve fibers. II. Dependence on spontaneous activity and relation to cochlear nonlinearity. J Neurophysiol 100:2899–2906

VON BISMARCK G (1967) The sound pressure transformation function from free-field to the eardrum of chinchilla. (Master's Dissertation, Dept. of Electrical Engineering, Massachusetts Institute of Technology), pp 1-93. Cambridge, MA.

WILSON JP, BRUNS V (1983) Middle-ear mechanics in the CF-bat Rhinolophus ferrumequinum. Hear Res 10:1–13